Reaction-Controlled Binder Burnout of Ceramic Multilayer Capacitors

H. Verweij* and W. H. M. Bruggink

Philips Research Laboratories, 5600JA Eindhoven, The Netherlands

Reaction-controlled binder burnout of ceramic multilayer capacitors (CMCs) is conducted in a series of small-scale experiments. The burnout process is followed by monitoring the weight of the CMCs. The observed maximum weight loss rate, obtained with a conventional linear heating process, is used to design a weight–time program for a reaction-controlled process. In this process the actual CMC weight is controlled to closely follow the weight program by means of continuous control with the batch temperature. The advantages of this procedure are discussed. The results of the present study, although being restricted to oxidative burnout of a special product, are thought to be of some use for other ceramic burnout situations. The relevant parts of controller design are discussed together with some comments on scale-up. [Key words: binders, thermogravimetry, processing, ceramic multilayer capacitors, zirconia.]

I. Introduction

BINDER burnout is a critical and time-consuming part of the ceramic multilayer capacitor (CMC) production process. In this process tapes with a typical thickness of 50 μm are made from a suspension containing dielectric powder and a binder. On these tapes an electrode pattern of, for instance, Pd/PdO or Pd/Ag is screened. Various tapes are carefully stacked and pressed together at a slightly elevated temperature. The resulting plates are carved and broken to obtain the separate green products. After binder burnout the products are sintered in an oxidizing atmosphere and provided with end terminations.

CMC binder burnout typically occurs in air in a prefiring furnace with a temperature–time schedule as follows: Initially the temperature is raised quickly to a level where binder burnout starts and is subsequently programmed at a very low constant rate up to a level where burnout is almost complete. An example of such a temperature–time schedule can be found in Fig. 1. The rate of temperature increase is kept very low during burnout to avoid the formation of cracks, blisters, and bubbles and the occurrence of delamination. An important part of the CMC burnout process is exothermic, while the catalytic activity of the Pd/PdO may give a considerable enhancement of reaction speed. One consequence of this is that the binder burnout process by itself may generate enough heat to cause a self-propagating reaction. Binder burnout is generally accompanied by a continuous weight decrease, which means that weight is a good measure for the stage of burnout. The weight–time curve for the products during temperature linear burnout will generally be S-shaped as a result of the superposition of increase of burnout rate and binder depletion with temperature.

Binder burnout occurs in many ceramic fabrication processes but fundamental studies are scarce.[1-6] Serious problems with binder removal of complex injection-molded ceramic
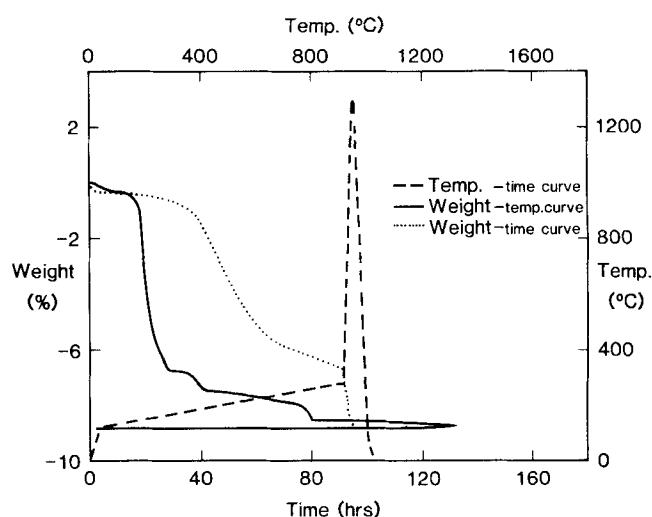
Fig. 1. Overall temperature–time, weight–time, and weight–temperature curves for conventional binder burnout and sintering of CMCs.

parts have recently triggered a research program at the MIT Materials Processing Center while proposals for solutions to the problems resulted in a series of patents and papers. Examples are to be found in Refs. 7–18 and 19–20; a review has been given in Ref. 21. The chemistry of binder burnout for a single type of organic binder is already very complex. Organic polymers may melt into low-viscosity fluids, decompose into monomers, or degrade thermally or under the influence of atmospheric components. Organic compounds may be completely burned by oxygen or a carbonaceous residue may remain present up to high temperatures.[1] In the description of the burnout process in terms of spatial distribution of organics two extremes are possible.[5] In the first, the reaction occurs at the surface of a shrinking core of binder phase. In the second, the binder burns out homogeneously throughout the structure. The real binder burnout process will always be in between the two extremes. If the shrinking core mechanism is dominant, extensive pressure buildup of gaseous reaction products at the binder phase surface and large volume differences between the binder phase and the burnout part should be avoided. If the homogeneous mechanism is dominant, there is a risk of internal bubble or blister formation and of capillary transport of small particles to the surface of the product. The latter mechanism is mentioned as a cause of subsequent crack formation during sintering due to large shrinkage differences between the surface and the interior.[15]

In Refs. 7, 9, 14, and 16 it is proposed to surround moldings with an inorganic powder to absorb low-viscosity liquid binder components during burnout while in Ref. 8 it is shown that "boiling" of binder components can be avoided by increasing the total atmospheric pressure in the furnace during burnout. In Ref. 10 it is proposed to degrade binder polymer by means of UV radiation while Ref. 11 reports on the use of a burnout atmosphere with a partial oxygen pressure higher

than that of normal air. It is mentioned there that the surface region of moldings is generally more dense than the bulk and that high oxygen partial pressures have the advantage that the surface structure is burnt open so that internal pressure buildup is diminished. The proposal of Ref. 11 seems to promote the shrinking core mechanism and may be interesting for CMC burnout if the velocity of the (exothermic) reaction can be kept under control. In Ref. 13 it is proposed to program the total furnace pressure such that the volume production rate of gaseous binder decomposition products is constant. In Ref. 15 it is proposed to diminish the fraction of fine particles in the ceramic powder used, to avoid migration of these particles to the surface by low-viscosity binder components. It is not certain that this mechanism is also present in burnout of CMCs which generally have a low binder content and a considerable green porosity. In Ref. 17 it is proposed to make the furnace atmosphere composition equal to that of the gaseous burnout products.

All the proposals of Refs. 7–11 and 13–17 aim to interfere with the chemistry of burnout with the inherent risk of conflicts with other processing demands. This is different for the proposals of Refs. 12 and 18–20, in which an attempt is made to directly improve process control with a given binder formulation and burnout situation. Various kinds of feedback control of the furnace temperature using weight sensoring are proposed. In Ref. 12 the rate of weight decrease, dW/dt, is monitored and translated into a rate of temperature increase such that dW/dt remains constant. No details of the control method are given, but from the examples it can be concluded that a discontinuous method is used. In Ref. 13 the inventors mention that temperature control is unstable and the method as such does not support the possibility of furnace temperature decrease which can be necessary for exothermic burnout. In Refs. 19 and 20 weight monitoring is used to stop temperature increase if a certain preset dW/dt is exceeded and reductions of burnout time of 50% are claimed. The method of Refs. 19 and 20, again, does not allow for furnace temperature decreases and the discontinuous control algorithm that is used appears to result in severe oscillations in the actual dW/dt. One of the problems with conventional slow-temperature linear burnout is that for practical reasons the total temperature range taken is generally much larger than the actual critical range where burnout occurs. This means that a lot of time is spent in slow heating while nothing happens. Narrowing down the slow heating rate range can be risky because of the limited reproducibility of the furnace temperature where burnout rates become significant and of the temperature where burnout is complete. An obvious advantage of methods such as mentioned in Refs. 19 and 20 is that the region of slow temperature increase is neatly adapted to the actual burnout situation.

In Ref. 18 a proposal is made for a CMC binder burnout process in oxidizing atmospheres in which the weight is controlled to follow a predefined weight–time program closely. This is accomplished by continuous PI (proportional with integrative action) control of the weight signal by means of the furnace temperature in an adaptive cascade configuration, to be explained in Section II. The control algorithm is designed such that the occurrence of both exothermic and endothermic reactions is kept under control, eventually resulting in temperature decreases as well as increases during burnout. It is the purpose of the present paper to describe the method together with instrumental details in a series of experiments on production samples. A special emphasis is placed on the description of the critical components of controller design.

II. Experimental Procedure

(1) General

Typical green CMC production samples were kindly supplied by the Philips Components division and made as fol-

lows: Foils with a thickness of about 50 μm were obtained by continuous casting of a slip containing the ceramic powder and a poly(vinyl alcohol) binder. On these foils an electrode pattern of Pd is screened and the various foils are piled up in the proper way and pressed together. The resulting plates are broken in order to obtain the separate capacitors with an average ceramic green density of 61% and a binder content of about 8%. All binder burnout experiments were performed in a thermogravimetric setup of the single-furnace type. General details of this setup are given in Ref. 22. The furnace atmosphere at the beginning of the experiments was air or pure O_2 at an absolute pressure of 101.325 kPa. Partial oxygen pressures in the gas stream at the input and the output of the furnace were measured with ZrO_2 sensors. All gases used in the experiments were prepurified in a continuous gas purifier with molecular sieves to remove polar gas impurities. Control of conventional process parameters was made as stable as possible in order to be able to highlight the intrinsic stability of the reaction control experiments performed.

Sample temperature control over the complete temperature range of the process was performed by direct digital adaptive PI(D) cascade control. This implied that sample temperature set-point control was performed by using a controller, with proportional (P), integrative (I), and derivative (D) action, providing a set point for second PI element temperature controller that in its turn generated a set point for the furnace power. The PI(D) parameters of both controllers were automatically adapted to the sample and element temperatures in order to obtain optimal control at all process temperatures. The optimal I and D parameters depend on temperature as the furnace time constants decrease considerably with increasing temperature while the optimal proportional band value is temperature dependent because of a variation in furnace power characteristics. More details on the control configuration are given in the Appendix. During the experiments the temperature set-point conformity was better than 2°C on the slopes with almost no overshoot at the initial part of the levels; the stability on the set-point levels was about 0.1°C.

Gas flows were controlled with a stability of 0.25% and an accuracy of 1%. The absolute pressure was controlled with a stability of about 10 Pa and an absolute accuracy of 0.5%. All process input signals were filtered using first-order lags with a time constant of 3 s. Gas purification, flow, and pressure control are standard features on the setup used and are probably very critical for the present reaction control experiments.

(2) Initial Binder Burnout Experiments

The starting point of the experiments was a conventional binder burnout procedure, carried out in air with flow rate of 10 sccm (standard cm^3/min) and a temperature program as follows: 30°C/h up to 110°C, 5°C/h up to 125°C, 1.786°C/h up to 275°C, and 2 h constant. Sintering was done in air directly after the burnout process without cooling down with 288.6°C/h up to 1285°C, 0.75 h constant, and cooling down to room temperature with −288.6°C/h. The products obtained were subjected to standard tests of specifications and lifetime properties and polished sections were inspected by light microscopy; no failures were detected. The tempeature–time schedule, together with the weight–time and weight–temperature curves obtained, are represented in Fig. 1, from which it can be observed that most of the binder burnout occurs between 125° and 275°C with some release of volatile components in the initial temperature path below 125°C. The maximum weight loss rate of about 0.2%/°C = 0.36%/h occurs at 188°C. During binder burnout and subsequent heating the Pd electrodes oxidize to PdO. The weight decrease just before 800°C is ascribed to the thermal reduction of PdO back to Pd. After determination of the conventional burnout behavior, a number of reaction control experiments were performed in which the control conditions were optimized. In these experiments the burnout process was started up in the same temperature–time schedule as used before and reaction

control of the sample weight was initiated as soon as weight loss of 0.5%, where burnout reactions became detectable, was reached. During reaction control the weight loss percentage was controlled to decrease linearly at a rate of $-0.36\%/h$ using PI control of the sample weight by means of the sample temperature. More details of the control configuration and control loop (re)initiation are given in the Appendix. Optimum values of 20% and 14.4 min for the proportional band (X_0) and integrative action time constant (I_0), respectively, were obtained as usual from the critical proportional band and the oscillation period for slightly unstable P control using the Ziegler–Nichols rules.[23] Attempts to apply full PID control with an "optimal" parameter set of $X_0 = 18\%$, $I_0 = 9$ min, and $D_0 = 108$ s were only occasionally successful because of control initiation problems. During reaction control the sample temperature control mode was switched bumplessly from PID to PI and vice versa afterward to avoid excessive temperature oscillations caused by amplification of sample temperature set-point noise during reaction control.

Reaction control was terminated when the sample temperature set point reached the level of 275°C, where the normal temperature program was continued. Again the products obtained after sintering were subjected to standard tests and no failures were detected. Examples of a temperature–time curve, together with weight–time and weight–temperature curves obtained with optimal PI reaction control, are represented in Figs. 2 and 3. The total process time appears to be reduced from more than 100 h to less than 40 h. The actual weight signal is observed to follow the programmed weight set point to within 0.04%, even during reaction control initiation. The temperature–time curve shows two tuning peaks at the beginning of reaction control. The occurrence of these peaks which are damped out effectively is caused by the fact that the weight loss rate at reaction control initiation is not equal to the programmed rate of $-0.36\%/h$. After tuning in, the temperature is observed to become lower for some time, which can be ascribed to the exothermic nature of the burnout reaction. The reaction-controlled burnout appears to occur with only a moderate increase in temperature. If binder depletion becomes significant, the temperature rises rapidly and the reaction control process is terminated if a sample temperature set point of 275°C is reached.

A further reduction of total process time was obtained by modification of the initial part of the temperature program. The 5°C/h and 1.786°C/h slopes were omitted and reaction control was directly activated on a 30°C/h temperature set-

Fig. 3. Expanded temperature–time, weight–time, and weight–temperature curves for reaction-controlled binder burnout and sintering of CMCs together with the weight set-point program (thin drawn line).

point slope without any problems. The level of 2 h constant at 275°C was omitted too, and reaction control was terminated at 500°C, which is below the temperature where PdO decomposition starts. It also proved possible to perform reaction-controlled binder burnout in a pure oxygen atmosphere. An example of curves obtained in such a process is given in Fig. 4. The temperature–time curve for reaction-controlled burnout in O_2 shows an almost zero slope region where the burnout reaction is self-propagating at a constant speed. Conventional burnout with a slowly increasing temperature results in a self-accelerating process in this situation.

(3) Reaction-Controlled Binder Burnout of Critical Production Samples

The method of reaction-controlled binder burnout as presented above was tested further with another set of CMC production samples in which burnout appeared to be very critical. It was observed that in these samples a severe surface crack formation occurred that was most clearly visible just after burnout. Inspection of the conventional burnout process indicated that sudden exothermic reactions occurred. An example of the process curves is given in Fig. 5; the observed fluctuations in the oxygen partial pressure $(p(O_2))$ in the furnace output gas stream may be connected with an irregular reaction behavior such as the formation of microcracks or local delaminations that influence the reaction kinetics. It
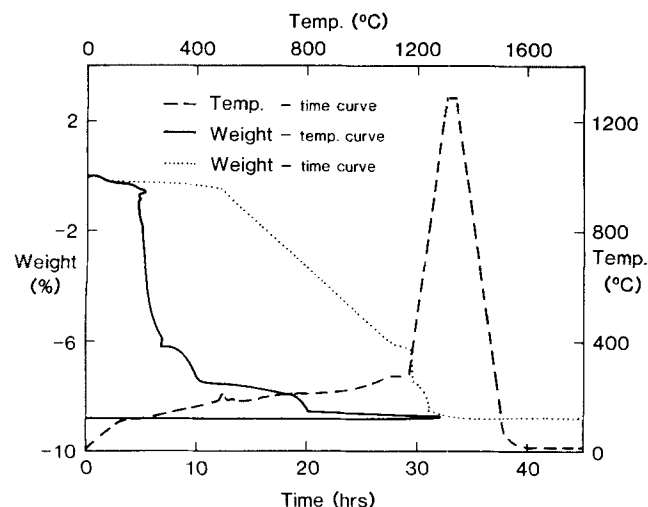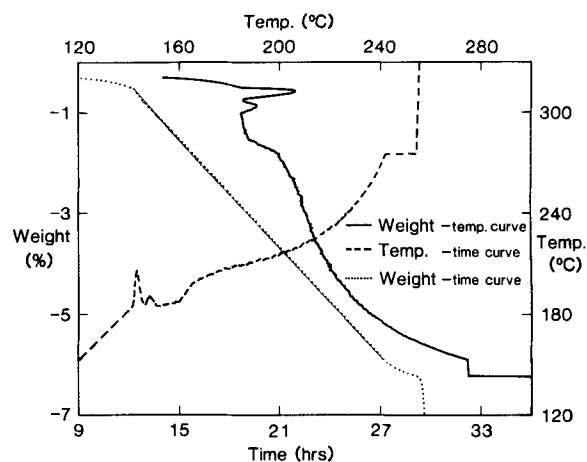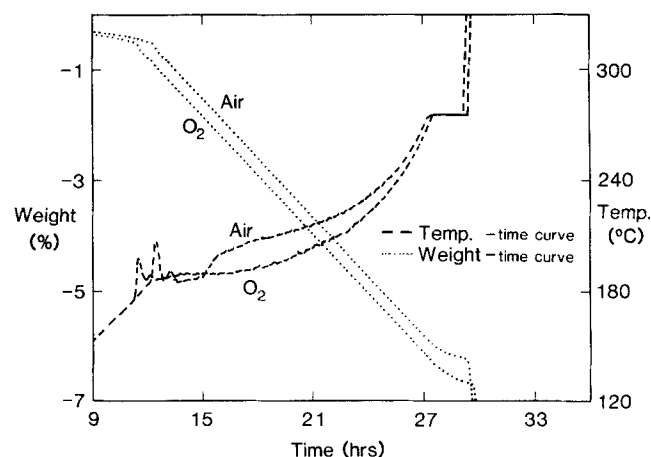

Fig. 2. Overall temperature–time, weight–time, and weight–temperature curves for reaction-controlled binder burnout and sintering of CMCs.

Fig. 4. Overall temperature–time, weight–time, and weight–temperature cuves for reaction-controlled binder burnout and sintering of CMCs in pure O_2.
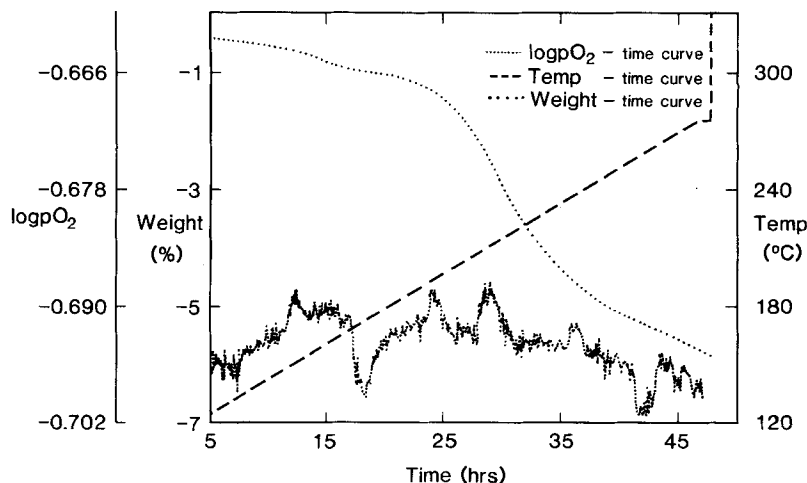
Fig. 5. Expanded temperature–time, weight–time, and $\log p(O_2)$–time curves for conventional binder burnout of critical CMCs in pure air.

was found that the reaction control procedure as described in the preceding section gave problems in the initial stage of the reaction control process. The fact that the weight loss rate at reaction control initiation was not equal to the programmed rate of $-0.36\%/h$ proved to be detrimental here. This problem could be solved, however, by using a multistep weight–time program for reaction control with gradually increasing weight loss rates. An example of process curves obtained with this multistep program is given in Fig. 6, where it can also be observed that the $p(O_2)$ fluctuations have diminished. A smooth weight–time program probably would have diminished the temperature fluctuations but required control software, dedicated to this specific problem.

III. Discussion and Conclusions

The small-scale experiments of the present study show that it is in principle possible to apply reaction control of oxidative binder burnout of CMCs while application of the method to other systems seems feasible. The total burnout time can be reduced considerably and tuning and control loop activation can be made such that the reaction rate varies gradually with time and never exceeds a certain limit. No special atmosphere or atmosphere control is necessary, but it is shown that it is possible to keep the process under control with pure O_2

or probably even more oxidizing or other reactive atmospheres. The control configuration is certainly more complex than for temperature-programmed systems and it should be realized that practical applications would be beyond reach if the costs of digital control equipment had not decreased so drastically. An additional argument is found in the considerable value of a complete production batch, justifying an investment in advanced control equipment with a diminished risk of explosive burnout. The experimentally obtained control parameters for the reaction control loop are characteristic for the green product samples investigated and do not depend much on the specifications of the control system. This is a consequence of the use of a cascade system in which the reaction control is by the sample temperature. The reaction control loop as such will not be drastically different for large-scale systems with a comparable configuration, as the coupling between binder burnout and temperature will be roughly the same. The differences are in temperature control dynamics, which may possibly have the consequence of a different reaction control initiation procedure. It was found in the present investigations that a good reaction control set-point conformity is easily obtained and that "tight" control in which the control parameters are near-critical is not necessary. This means that the reaction control parameters can be taken such that a considerable spread in product and binder
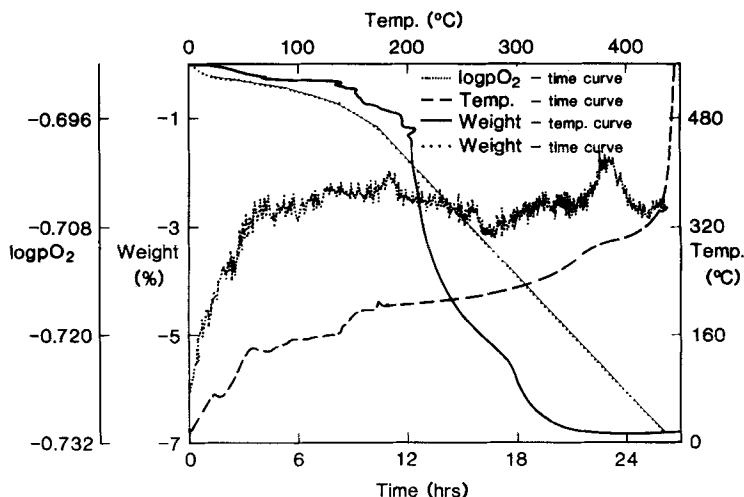

Fig. 6. Expanded temperature–time, weight–time, and weight–temperature curves for reaction-controlled binder burnout and sintering of CMCs together with the weight set-point program (thin drawn line).

burnout properties can be allowed without the need for reoptimization. Another reason that the reaction control parameters should not be too tight is the fact that in normal burnout systems process parameters such as gas pressure, flow rate, and furnace loading may not all be reproducible or under complete control.

The present approach ensures that an optimum temperature–time schedule is obtained automatically for each batch. The average burnout temperature is kept as low as possible so that the formation of unwanted carbonaceous residue is avoided as much as possible, while the risk of crack formation due to thermal expansion differences is minimized. Knowledge of details about the physics and chemistry of the binders and their burnout process is not necessary but a study of this might be interesting to construct more refined reaction control set-point programs. If a good model picture is obtained for the burnout process, it might be possible to calculate weight–time programs in which the internal gas pressure built up is always kept at an acceptable level. The CMC burnout process probably occurs layer by layer as the binders do no melt at the processing temperatures used. This means that the burnout process is comparable to shrinking core mechanism, so that a linear weight–time program can be accepted as a first attempt. For more complex shapes it is highly possible that some nonlinear, continuous weight–time program will give optimum results.

There is an essential difference between preprogramming an "ideal" temperature program and programming the reaction itself. In practical situations there will always be process perturbations occurring between the sample temperature and the burnout process. In temperature-controlled burnout these perturbations may influence the process locally in an uncontrolled way; in the reaction control mode they are "tuned away." The short-term fluctuations during steady-state reaction control on the temperature–time curves of Figs. 2 to 6 can be regarded as the result of intercepted process perturbations. An important practical consequence of reaction control by means of weight is that weight sensoring is generally very reliable, reproducible, and very accurate. It can be applied to large-scale processes in which simple load cells can be used. Reliability and reproducibility of thermocouples is less important and considerable drifts in calibration can be allowed. It is thought that the method can be implemented on existing burnout systems where the major effort will probably have to be put into the implementation of the control software. In the present experiments the complete burnout and sintering process were combined in one furnace system and it could be worthwhile considering this combination for a large-scale system, possibly making use of adaptive control.

APPENDIX

Control Loop Details and (Re)initiation Procedures

A simplified diagram of the cascade control configuration for both conventional temperature control and reaction control is given in Fig. A1. All feedback loops of the entire reaction control system were implemented with the so-called "ideal" PID algorithm:

$$Y_n = C_n \left(W_n + \int_{t=0}^{t=t} W_n/I_n\, dt + D_n\, dW_n/dt \right)(100/X_n)$$

$$= (C_n W_n + R_n + V_n)(100/X_n) \qquad (A-1)$$

in which $n = 0$ for the reaction controller, 1 for the sample temperature controller, and 2 for the element temperature controller, and C_n is the control mode (1 for normal and -1 for inverse control), Y_n the controller output signal, W_n the deviation of the controlled variable, I_n the integrative action time constant, t the process time, D_n the derivative action time constant, and X_n the proportional band in percent.
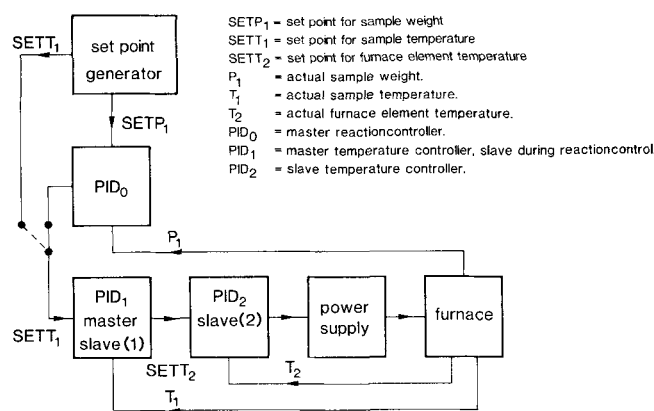

Fig. A1. Simplified diagram of the cascade control configuration for both conventional temperature control and reaction control. The switch is in the position for reaction control.

The control mode C_n is -1 for temperature control as usual and $+1$ for the present reaction control situation. Other reaction control situations are conceivable in which $C_0 = -1$. In the remainder of the discussion C_0 is kept general. The values of X, I, and D can be made to adapt to the actual values of the process variables, provided that the adaptation functions vary slowly compared to the process fluctuations. The integrative and derivative action parts of the PID algorithm are indicated further as R_n and V_n. The operation of the PID algorithm is straightforward except for the initiation and reinitiation procedures during switchover of the control modes to be discussed below. If the control process is stable with only minor set-point deviations, the PID controller output is mainly determined by the actual value of R_n. The $t = 0$ values of R_n can be taken as zero as usual, as the process generally starts at room temperature in normal temperature control mode.

At the stages of initiation and termination of reaction control the values of R_n have to be reinitiated for several reasons to avoid a complete loss of control. A detailed inspection of the control algorithm resulted in the following procedures:

(1) At the occurrence of reaction control loop initiation the value of R_0 is calculated such that the sample temperature set point becomes equal to the programmed set point $SETT_1$ just before reaction control initiation:

$$R_0 = X_0(SETT_1)/100 - C_0 W_0 - V_0' + C_0 S_0 D_0$$

in which S_0 is the initial programmed reaction control weight loss rate and V_0' is the derivative action of the reaction controller, obtained by letting it run as a dummy controller with a fixed-weight set point during conventional temperature control.

(2) If reaction control is active, $C_0 W_0$ is negative, and R_0 becomes 0, the value of R_0 is reinitiated such that the sample temperature set point becomes equal to the actual sample temperature:

$$R_0 = X_0 T_1/100 - C_0 W_0 - V_0$$

This reinitiation is useful to reduce dead process time if, for instance, during turning in, the reaction is completely stopped because of a large temperature decrease.

(3) At the occurrence of reaction control loop initiation or termination, the value of R_1 is reinitiated such that the element temperature set point becomes equal to the programmed set point $SETT_2$ just before reaction control initiation:

$$R_1 = X_1(SETT_2)/100 + W_1 - V_1$$

This procedure also allows for a discontinuous change of X_1, I_1, and D_1 in order to be able, for instance, to switch from PID to PI sample temperature control and vice versa, as mentioned in Section II.

(4) If W_1 is negative and R_1 becomes 0, the value of R_1 is reinitiated such that the element temperature set point becomes equal to the actual element temperature:

$$R_1 = X_1 T_2/100 + W_1 - V_1$$

This reinitiation is useful to reduce dead process time if, for instance, during tuning in, the furnace power was zeroed.

In addition, the usual measures are taken to avoid excessive windup of R_n. The reinitiation procedures mentioned require an interaction between the various control loops that is probably difficult to implement on analog systems.

References

[1]S. Strijbos, "Burning-Out of a Carbonaceous Residue from a Porous Body," *Chem. Eng. Sci.,* **28,** 205–13 (1973).

[2]C. Dong, "Binder Burnout in Ceramics," MIT Ceramic Processing Research Laboratory Report 80, Building No. 12, Massachusetts Institute of Technology Materials Processing Center, Cambridge, MA, 1987.

[3]M. J. Cima and J. A. Lewis, "Chemical Effects Leading to Residual Carbon during Binder Removal from Ceramic Greenware," MIT Ceramics Processing Research Laboratory Report 81, Building No. 12, Massachusetts Institute of Technology Materials Processing Center, Cambridge, MA, 1987.

[4]R. J. Higgins, "The Chemistry of Carbon Formation during Binder Burnout in Ceramics," MIT Ceramics Processing Research Laboratory Report 88, Building No. 12, Massachusetts Institute of Technology Materials Processing Center, Cambridge, MA, 1987.

[5]P. Calvert and M. J. Cima, "Theoretical Models for Binder Burnout," MIT Ceramics Processing Research Laboratory Report 91, Building No. 12, Massachusetts Institute of Technology Materials Processing Center, Cambridge, MA, 1988.

[6]M. J. Cima, J. A. Lewis, and A. D. Devoe, "Binder Distribution in Ceramic Greenware during Thermolysis," MIT Ceramics Processing Research Laboratory Report 92, Building No. 12, Massachusetts Institute of Technology Materials Processing Center, Cambridge, MA, 1988.

[7]R. Schreiber, O. Vogt, and R. Wosnitzka, "Heat Treatment of Ceramic Moldings," DDR Pat. No. 142330, 1980.

[8]R. E. Wiech, "Method and Means for Removing Binder from a Green Body," European Pat. No. 0032404, 1981.

[9]M. Ikejima and T. Imai, "Production Method of Ceramic Bodies," Jpn. Pat. No. 141462 337-342, 1984.

[10]K. Iwata, T. Nishimoto, and H. Takahashi, "Compositions for Ceramic Moldings and a Debindering Method for Ceramic Molding Compositions," Jpn. Pat. No. 199570 415-417, 1984.

[11]R. E. M. Gilissen, A. G. Smolders, and J. F. C. Cooymans, "Method for Binder Removal from a Green Powder Compact," Belg. Pat. No. 903308, 1985.

[12]T. Sakai, M. Inouè, Y. Kihara, and Y. Kawabata, "Debindering Method for Ceramic Green Moldings," Jpn. Pat. No. 215577 461-463, 1985.

[13]T. Sakai, M. Inouè, Y. Kihara, and Y. Kawabata, "Debindering Method for Ceramic Green Moldings," Jpn. Pat. No. 215578 465-467, 1985.

[14]W. Tanikawa and N. Kurata, "Debindering Materials for Ceramic Moldings, Their Production Method, Their Use and a Debindering Apparatus in Which a Full Profit Is Made of Their Properties," Jpn. Pat. No. 251173 587-593, 1985.

[15]G. Bandyopadhyay, K.W. French, L. J. Bowen, and J.T. Neil, "Method for Fabricating of Large Cross Section Injection Molded Ceramic Shapes," European Pat. No. 0196600, 1986.

[16]S. Katō, "Debindering Method for Ceramic Moldings," Jpn. Pat. No. 53147 249-254, 1986.

[17]T. Ando, "Production Method for Ceramic Parts," Jpn. Pat. No. 83682 531-533, 1986.

[18]H. Verweij and W. H. M. Bruggink, "Apparatus and Method for Removal of Organic Binder from a Green Ceramic Powder Compact," Dutch Pat. Application No. PHN 12.387, 1988.

[19]A. Johnsson, E. Carlström, L. Hermansson, and R. Carlsson, "Minimisation of the Extraction Time for Injection Molded Ceramics," *Proc. Br. Ceram. Soc.,* **33,** 139–47 (1983).

[20]A. Johnsson, E. Carlström, L. Hermansson, and R. Carlsson, "Rate-Controlled Extraction Unit for Removal of Organic Binders from Injection-Molded Ceramics," *Mater. Sci. Monogr.,* **16,** 767–72 (1983).

[21]M. J. Edirisinghe and J. R. G. Evans, "Review: Fabrication of Engineering Ceramics by Injection Molding. II, Techniques," *Int. J. High Technol. Ceram.,* **2** [4] 249–78 (1986).

[22]H. Verweij and W. H. M. Bruggink, "Precision Determination of the Stoichiometry Parameter x of $YBa_2Cu_3O_x$," *J. Phys. Chem. Solids,* **49** [9] 1063–69 (1988).

[23]J. G. Ziegler and N. B. Nichols, *Trans. ASME,* "Optimum Settings for Automatic Controllers," **64** [11] 759–68 (1942).　　□